



# Study of $\Lambda^+ c$ Semileptonic Decays. Search for Time-Reversal Violation

Rola Mostafa

## ► To cite this version:

Rola Mostafa. Study of  $\Lambda^+ c$  Semileptonic Decays. Search for Time-Reversal Violation. High Energy Physics - Experiment [hep-ex]. 2015. dumas-01228678

**HAL Id: dumas-01228678**

**<https://dumas.ccsd.cnrs.fr/dumas-01228678>**

Submitted on 9 Dec 2015

**HAL** is a multi-disciplinary open access archive for the deposit and dissemination of scientific research documents, whether they are published or not. The documents may come from teaching and research institutions in France or abroad, or from public or private research centers.

L'archive ouverte pluridisciplinaire **HAL**, est destinée au dépôt et à la diffusion de documents scientifiques de niveau recherche, publiés ou non, émanant des établissements d'enseignement et de recherche français ou étrangers, des laboratoires publics ou privés.



Distributed under a Creative Commons Attribution - NonCommercial - NoDerivatives| 4.0 International License



UFR Sciences et Technologies



Laboratoire de Physique Corpusculaire  
de Clermont-Ferrand

# **MASTER SCIENCES DE LA MATIERE DEUXIEME ANNEE**

**SPECIALITE : Physique des Particules**

**RAPPORT DE STAGE**

## ***Study of $\Lambda_c^+$ Semileptonic Decays Search for Time-Reversal Violation***

par

**Rola MOSTAFA**

Responsable(s) de stage : **Ziad AJALTOUNI**



**Juin 2015**

# Contents

<b>Introduction</b>	<b>3</b>
<b>1 Discrete Symmetries</b>	<b>4</b>
1.1 CPT Symmetry . . . . .	4
1.2 CP Symmetry . . . . .	4
1.3 Time-Reversal T . . . . .	5
<b>2 Phenomenological Study of the Decay Channel <math>\Lambda_c^+ \rightarrow \Lambda \mu^+ \nu_\mu</math></b>	<b>7</b>
2.1 Introduction to Polarization . . . . .	7
2.1.1 Density Matrix of a Quantum System . . . . .	7
2.1.2 Definition of Polarization . . . . .	7
2.1.3 Polarization in Decay Processes . . . . .	9
2.2 Kinematics . . . . .	9
2.2.1 Choice of the Frames . . . . .	9
2.2.2 T-odd Observables . . . . .	11
2.3 Calculation of the Angular Distributions . . . . .	12
2.3.1 Initial Resonance Decay: $\Lambda_c^+(M_i) \rightarrow \Lambda(\lambda_1)W^+(\lambda_2)$ . . . . .	12
2.3.2 Decay 1: $\Lambda(\lambda_1) \rightarrow P(\lambda_3)\pi^-(\lambda_4)$ . . . . .	14
2.3.3 Decay 2: $W^+(\lambda_2) \rightarrow \mu^+(\lambda_5)\nu_\mu(\lambda_6)$ . . . . .	15
<b>3 Simulations</b>	<b>18</b>
3.1 Kinematics of the Decay $\Lambda_c^+ \rightarrow \Lambda \mu^+ \nu_\mu$ . . . . .	18
3.1.1 Three-Body Decay Process . . . . .	18
3.2 Monte-Carlo Simulations . . . . .	20
3.2.1 Step 1 . . . . .	20
3.2.2 Step 2 . . . . .	21
3.2.3 Step 3 . . . . .	22

Conclusion	28
Bibliography	29

# Introduction

To which degree are the physical laws invariant under Time-Reversal transformation?

Until 1964, Time-Reversal symmetry was naively assumed to be conserved in weak interactions as well as in electromagnetic and strong interactions. Therefore the discovery of CP violation was completely unexpected when, in 1964, Val Fitch, Jim Cronin and other collaborators observed this phenomenon for the first time in the weak decays of neutral kaons. This discovery came out with a remarkable thing that has to do with Time-Reversal symmetry. According to the logic of CPT Theorem, one of the most basic concepts of particle physics, the violation of CP leads us to admit the violation of Time-Reversal symmetry in an indirect way.

Independently of CP violation, weak decays of charmed baryons like  $\Lambda_c^+$  into  $\Lambda\mu^+\nu_\mu$ , where the produced intermediate resonances are polarized, offer interesting opportunity to perform tests of Time-Reversal invariance in a direct way.

Our aim in this training is to look for a Time-Reversal violation in the weak semileptonic decay of the heavy baryon  $\Lambda_c^+$ . In chapter 1, a brief introduction to the main discrete symmetries involved in our work is given. Next, there will be a phenomenological study of the decay through which calculations of the angular distributions of the initial decays  $\Lambda_c^+ \rightarrow \Lambda W^+$  are done, and similar ones for the hadronic and leptonic decay products of those intermediate resonances are made based on the helicity formalism of Jacob-Wick and Jackson. Finally, in chapter 3, a purely kinematic study is performed followed by a simulation of the angular distributions by the method of Monte-Carlo.

# Chapter 1

## Discrete Symmetries

Symmetries are a fundamental topic of interest in modern particle physics. They are classified mainly in two categories: Continuous and Discrete. As an example of continuous symmetries, we have time translation, space translation and space rotation. Beside these continuous symmetries, one has three important discrete symmetries: Charge Conjugation **C**, Parity **P** and Time-Reversal **T**. The Charge Conjugation transforms a particle into its antiparticle and vice versa ( $q \rightarrow -q$ ). The Parity inverts all spatial coordinates ( $\vec{r} \rightarrow -\vec{r}$ ) and all vector-momentum components ( $\vec{p} \rightarrow -\vec{p}$ ). The Time-Reversal reflects the time coordinate ( $t \rightarrow -t$ ) and the vector-momentum components ( $\vec{p} \rightarrow -\vec{p}$ ), while leaving  $\vec{r}$  unchanged. The focus of the present chapter centers on discrete symmetries; particularly, the Time-Reversal symmetry and the two composed discrete symmetries: **CP** and **CPT**.

### 1.1 CPT Symmetry

**CPT** symmetry is the combination of the three discrete symmetries: **C**, **P** and **T**. According to Lorentz invariance and the principle of locality in Quantum Field Theory, it is an exact symmetry of nature. A consequence of this symmetry conservation is that particle and antiparticle have the same mass and lifetime [1]. The **CPT** Theorem asserts that the results of all physical laws are invariant under the **CPT** transformation. In other words, the probability amplitudes will be the same before and after the transformation.

$$|\langle \psi_1 | H | \psi_2 \rangle|^2 = |\langle \psi_1^{CPT} | H | \psi_2^{CPT} \rangle^*|^2$$

### 1.2 CP Symmetry

**CP** symmetry combines **C** with **P**. The result of the CP transformation is a particle with an inverted charge turning in the opposite sense (Figure 1.1). It is not a perfect symmetry of nature since its violation was first discovered in 1964 by James Cronin, Val Fitch and other collaborators in the study of the decays of neutral kaon system ( $K^0$ ,  $\bar{K}^0$ ). This discovery has given us a possible explanation for why the universe appears to contain more matter than antimatter (A.Sakharov, 1966). **CP** symmetry violation was also seen in the B and D systems [2].

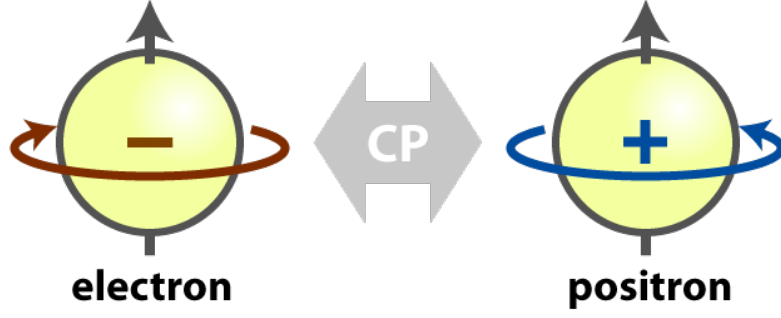


Figure 1.1: CP Symmetry

### 1.3 Time-Reversal $\mathbf{T}$

Time-Reversal transformation is represented by an operator  $\mathbf{T}$  that reflects  $t$  into  $-t$  and  $\vec{p}$  into  $-\vec{p}$  while leaving  $\vec{r}$  unchanged. By exchanging also the initial and final states, it represents a reversal of motion.

$$\mathbf{T} : t \rightarrow -t$$

Consider the Schrodinger equation for the state vector  $|\psi(\vec{r}, t)\rangle$ :

$$H|\psi(\vec{r}, t)\rangle = i\hbar \frac{\partial |\psi(\vec{r}, t)\rangle}{\partial t} \quad (1.1)$$

Applying the transformation  $t \rightarrow -t$  to both sides of the Schrodinger equation, we get:

$$H|\psi(\vec{r}, -t)\rangle = -i\hbar \frac{\partial |\psi(\vec{r}, -t)\rangle}{\partial t} \quad (1.2)$$

This is not the Schrodinger equation due to the presence of a minus sign. In order to return to the desired form of Schrodinger equation, we take the complex conjugate of equation (1.2). Therefore:

$$H|\psi^*(\vec{r}, -t)\rangle = +i\hbar \frac{\partial |\psi^*(\vec{r}, -t)\rangle}{\partial t} \quad (1.3)$$

with  $H = H^*$  since hamiltonian operator is hermitian.

We thus find again the standard form of the Schrodinger equation with:

$$\mathbf{T}|\psi(\vec{r}, t)\rangle = |\psi^*(\vec{r}, -t)\rangle \quad (1.4)$$

So we define in Quantum Mechanics a new operator, Time-Reversal  $\mathbf{T}$ , expressed as:

$$\mathbf{T} = UK \quad (Wigner, 1932) \quad (1.5)$$

where  $K$  is the complex conjugate operator and  $U$  is a unitary operator.

As a result, the Time-Reversal transformation is represented by an anti-unitary operator  $\mathbf{T}$ , different from the charge conjugation and parity transformation which are unitary operators. Some observables under Time Reversal transformation are shown in the Table 1.1 .

observable	$\mathbf{T}(\text{observable})$
$t$	$-t$
$\vec{r}$	$\vec{r}$
$\vec{p}$	$-\vec{p}$
$\vec{L}$	$-\vec{L}$
$\vec{S}$	$-\vec{S}$
$\vec{E}$	$\vec{E}$
$\vec{B}$	$-\vec{B}$

Table 1.1: Effect of Time-Reversal transformation on some observables

According to the logic of the **CPT** Theorem, the violation of one of the symmetries, either singly or combined, must be accompanied by a compensating violation of another symmetry in order to satisfy the requirements of the theorem. Therefore, **CP** symmetry violation implies the violation of **T** symmetry; this is a proof of *indirect violation* of **T** symmetry [3].

In our work, we are searching for a *direct violation* of **T** symmetry; particularly, in the weak semileptonic decay of the charmed baryon  $\Lambda_c^+$  (Figure 1.2).

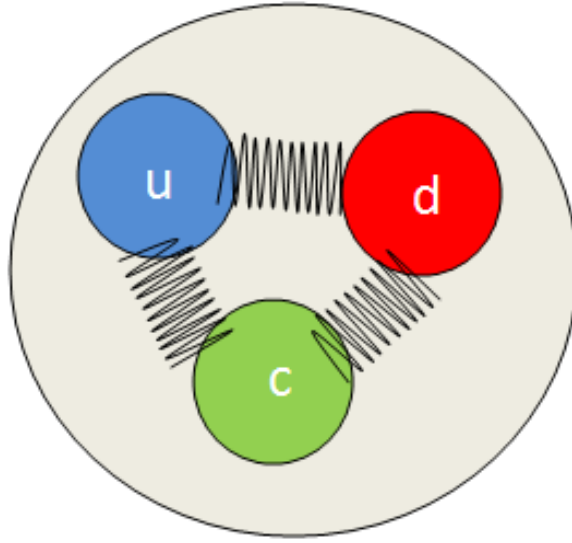


Figure 1.2:  $\Lambda_c^+$  Baryon



# Chapter 2

## Phenomenological Study of the Decay Channel $\Lambda_c^+ \rightarrow \Lambda \mu^+ \nu_\mu$

The  $\Lambda_c^+$  is the first charmed baryon to be discovered experimentally after the discovery of the charm quark. Its mass, lifetime and decay modes made it an interesting charmed system worthy to be studied. In this chapter, we are dealing with the theoretical aspect of the  $\Lambda_c^+$  physics; precisely, the angular distributions of both the intermediate states and the final particles with the approximation of the quasi two-body decay.

### 2.1 Introduction to Polarization

#### 2.1.1 Density Matrix of a Quantum System

A quantum system which may be in a number of different quantum states with various probabilities is said to be in a mixed state. In this case, the system is described by a (nxn) matrix  $\rho$  named density matrix with the following properties: [4, 5, 6]

- Normalization:  $Tr(\rho) = 1$
- Hermiticity:  $\rho = \rho^\dagger$
- Positivity:  $\rho_{ii} \geq 0$
- Schwartz Inequality:  $|\rho_{ij}|^2 \leq \sum \rho_{ii} \rho_{jj}$

#### 2.1.2 Definition of Polarization

The polarization vector  $\mathbf{P}$  of a particle of spin  $S$  is defined as the mean value of the spin  $\mathbf{S}$  given by the following relation:

$$\mathbf{P} = \frac{\langle \mathbf{S} \rangle}{S} = \frac{Tr(\rho \mathbf{S})}{S}$$

where  $\rho$  is the spin density matrix with dimension  $(2S+1) \times (2S+1)$ .

In cartesian coordinates, the polarization vector  $\mathbf{P}$  is written as:

$$\mathbf{P} = P_x \mathbf{X} + P_y \mathbf{Y} + P_z \mathbf{Z}$$

where  $|\mathbf{P}| = \sqrt{P_x^2 + P_y^2 + P_z^2}$  is the norm of the polarization vector which varies between 0 and 1; in other words, between a non polarized state (0) and a completely polarized state (1). The intermediate values represent partial polarization.

### Case of a spin 1/2 particle

For a spin 1/2 particle, the density matrix is a (2x2) matrix defined as follows:

$$\rho = \frac{1}{2}(I + \boldsymbol{\sigma} \cdot \mathbf{P}) = \begin{pmatrix} \rho_{++} & \rho_{+-} \\ \rho_{-+} & \rho_{--} \end{pmatrix}$$

where  $I$  is the (2x2) identity matrix and  $\boldsymbol{\sigma}$  are the Pauli matrices. We need 3 real parameters in order to define  $\rho$ :  $\rho_{++}$ ,  $\text{Re}(\rho_{+-})$  and  $\text{Im}(\rho_{+-})$ .

Making use of the explicit representation of the Pauli matrices, the density matrix becomes:

$$\rho = \frac{1}{2} \begin{pmatrix} 1 + P_z & P_x - iP_y \\ P_x + iP_y & 1 - P_z \end{pmatrix}$$

where  $\rho_{++}$  and  $\rho_{--}$  are the probabilities that the spin projection along the quantization axis is equal to +1/2 and -1/2 respectively.

One can deduce:

$$P_z = (\rho_{++} - \rho_{--}) \quad , \quad P_x = 2\text{Re}(\rho_{+-}) \quad , \quad P_y = -2\text{Im}(\rho_{+-})$$

Therefore, the knowledge of the density matrix elements enables us to obtain the components of the polarization vector  $\mathbf{P}$  [4, 5].

The projection of the polarization vector  $\mathbf{P}$  along any axis ( $\Delta$ ) is the degree of polarization along this axis and it is defined as follows:

$$P_\Delta = \frac{N(+1/2) - N(-1/2)}{N(+1/2) + N(-1/2)}$$

where:

$$\begin{cases} \frac{N(+1/2)}{N(+1/2) + N(-1/2)} : \text{probability of pure states with spin up along } \Delta \\ \frac{N(-1/2)}{N(+1/2) + N(-1/2)} : \text{probability of pure states with spin down along } \Delta \end{cases}$$

### Case of a spin 1 particle

Generalizing to a spin 1 particle, the density matrix is a (3x3) matrix defined as follows:

$$\rho = \begin{pmatrix} \rho_{11} & \rho_{10} & \rho_{1-1} \\ \rho_{01} & \rho_{00} & \rho_{0-1} \\ \rho_{-11} & \rho_{-10} & \rho_{-1-1} \end{pmatrix}$$

Here we need 8 real parameters in order to define  $\rho$ .

### 2.1.3 Polarization in Decay Processes

The basic principles of Quantum Mechanics allow us to deduce the polarization density matrix of the final system  $R_1 R_2$  of a resonance decay  $R_0 \rightarrow R_1 R_2$ , which is an essential ingredient to compute the polarization vector of each resonance:  $\rho^f = T^\dagger \rho^{R_0} T$ , where  $T$  is the transition matrix defined by the  $S$  matrix ( $S=1+iT$ ). The normalization of the matrix  $\rho^f$  is obtained by:  $Tr(\rho^f) = \frac{d\sigma}{d\Omega} = NW(\theta, \phi)$  where  $N$  being the normalization constant and  $\phi, \theta$  being the azimuthal and polar angles of the  $\Lambda$  in the  $\Lambda_c^+$  rest frame. Consequently, the polarization vector of any resonance  $R_i$  is defined by:

$$\mathbf{P}_i = \langle \mathbf{S}_i \rangle = \frac{Tr(\rho_i^f \mathbf{S}_i)}{Tr(\rho_i^f)}$$

where  $\rho_i^f$  is the polarization density matrix of the resonance  $R_i$  deduced from  $\rho^f$ .

As the final state is a composite system made out of two particles with different spins ( $S_1 = \frac{1}{2}, S_2 = 1$ ), each  $\rho_i^f$  will be obtained from the general expression of  $\rho^f$  by summing up over the degrees of freedom of the other resonance. Thanks to this method, we can obtain  $\rho^\Lambda$  and  $\rho^V$ . We apply the same method to the decay  $\Lambda_c^+ \rightarrow \Lambda W^+$  [3].

## 2.2 Kinematics

When a  $\Lambda_c^+$  is produced in the p-p collisions, it is assumed to be mainly produced by Strong Interactions and thus to be transversely polarized. It decays by weak interaction giving the intermediate resonance  $\Lambda$  and the virtual W-boson  $W^+$  which are both polarized. For our purpose, it is convenient to regard the semileptonic decay  $\Lambda_c^+ \rightarrow \Lambda \mu^+ \nu_\mu$  as a quasi two-body decay  $\Lambda_c^+ \rightarrow \Lambda W^+$  [7]. Then  $\Lambda$  decays into proton and pion and the virtual W-boson decays into muon and muon-neutrino.

$$\Lambda_c^+ \rightarrow \Lambda W^+ \rightarrow p \pi^- \mu^+ \nu_\mu$$

### 2.2.1 Choice of the Frames

#### $\Lambda_c^+$ Production Plane

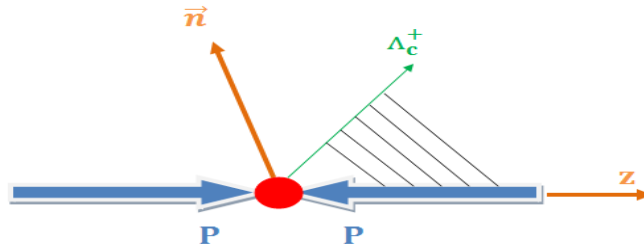


Figure 2.1: Production plane of  $\Lambda_c^+$

Let us define  $\vec{n}$  the normal vector to the production plane by the relation:

$$\vec{n} = \frac{\vec{p}_p \times \vec{p}_{\Lambda_c}}{|\vec{p}_p \times \vec{p}_{\Lambda_c}|}$$

where  $\vec{p}_p$  and  $\vec{p}_{\Lambda_c}$  are the vector-momentum of one of the incident protons and the vector-momentum of the  $\Lambda_c^+$  respectively in the standard frame of the LHCb detector (Oxyz) as shown in Figure 2.1 .

### $\Lambda_c^+$ Transversity Frame

Based on the assumption that the produced  $\Lambda_c^+$  in the p-p collisions could be transversely polarized, we define a new frame (Ox'y'z') such that:

- $\vec{Oz'}$ : it is orthogonal to the  $\Lambda_c^+$  production plane. So it is parallel to the normal vector  $\vec{n}$  and the unit vector  $\vec{e}_{z'} = \vec{n}$ . It is defined as the quantization axis in this reference frame.
- $\vec{Ox'}$ : it is parallel to the  $\vec{p}_p$  ;  $\vec{Ox'} = \vec{Oz}$  with the unit vector  $\vec{e}_{x'} = \frac{\vec{p}_p}{|\vec{p}_p|}$  .
- $\vec{Oy'} = \vec{Oz'} \times \vec{Ox'}$  and the unit vector  $\vec{e}_{y'} = \vec{e}_{z'} \times \vec{e}_{x'}$  .  
The  $\Lambda_c^+$  vector-momentum in the new frame is defined as  $\vec{p}_{\Lambda_c}' = (p_{\Lambda_c} \cos \theta_{\Lambda_c}, p_{\Lambda_c} \sin \theta_{\Lambda_c}, 0)$  where  $\theta_{\Lambda_c}$  is the angle between  $\vec{p}_{\Lambda_c}'$  and  $\vec{Ox'}$  and  $p_{\Lambda_c} = |\vec{p}_{\Lambda_c}|$ .

### $\Lambda_c^+$ Rest Frame

In order to calculate the angular distributions of  $\Lambda_c^+$  decay products, we construct the  $\Lambda_c^+$  rest frame ( $\Lambda_c^+$ XYZ) from (Ox'y'z') by a simple Lorentz Transformation  $\vec{\beta} = \frac{\vec{p}_{\Lambda_c}}{E_{\Lambda_c}}$  .  
where  $E_{\Lambda_c}$  is the  $\Lambda_c^+$  energy in the (Ox'y'z').

The quantization axis of the frame ( $\Lambda_c^+$ XYZ) is the same as that of (Ox'y'z');  $\vec{\Lambda_c^+Z} || \vec{Oz'} || \vec{n}$  .

### $\Lambda$ helicity Frame

The helicity state of the intermediate resonance  $\Lambda$  will serve as an initial value of the total angular momentum in the computation of the angular distributions of the final hadrons.

In order to calculate the angular distributions of  $\Lambda$  decay products, we have to move from the  $\Lambda_c^+$  rest frame to the  $\Lambda$  helicity frame ( $\Lambda X_1 Y_1 Z_1$ ) by:

- 1-Two successive rotations  $R_y(\theta)$  and  $R_z(\phi)$ ;  $\vec{\Lambda_c^+Z}$  becomes parallel to  $\vec{p}_{\Lambda}$ .
- 2-Lorentz boost  $\vec{\beta}_{\Lambda} = \frac{\vec{p}_{\Lambda}}{E_{\Lambda}}$  .

where  $\vec{p}_{\Lambda}$  and  $E_{\Lambda}$  are the vector-momentum and energy of  $\Lambda$  in  $\Lambda_c^+$  rest frame respectively.

### $W^+$ helicity Frame

The helicity state of the intermediate resonance  $W^+$  will serve also as an initial value of the total

angular momentum in the computation of the angular distributions of the final leptons.

In order to calculate the angular distributions of  $W^+$  decay products, we have to move from the  $\Lambda_c^+$  rest frame to the  $W^+$  helicity frame ( $W^+ X_2 Y_2 Z_2$ ) by:

1-Two successive rotations  $R_y(\pi - \theta)$  and  $R_z(\pi + \phi)$ ;  $\overrightarrow{\Lambda_c^+ Z}$  becomes parallel to  $\overrightarrow{p_W}$

2- Lorentz boost  $\beta_W = \frac{\overrightarrow{p_W}}{E_W}$ .

where  $\overrightarrow{p_W}$  and  $E_W$  are the vector-momentum and energy of  $W^+$  in  $\Lambda_c^+$  rest frame respectively.

In the  $\Lambda_c^+$  rest frame we define the unit vectors for each resonance basis as follows:

- $\vec{e}_L = \frac{\vec{p}}{|\vec{p}|}$  where  $\vec{p} = \overrightarrow{p_\Lambda}$  or  $\vec{p} = \overrightarrow{p_W}$ .
- $\vec{e}_T = \frac{\vec{e}_z \times \vec{e}_L}{|\vec{e}_z \times \vec{e}_L|}$ .
- $\vec{e}_N = \vec{e}_T \times \vec{e}_L$ .

The polarization vector for each resonance in its own rest frame can be expressed as:

$$\mathbf{P} = P_L \mathbf{L} + P_N \mathbf{N} + P_T \mathbf{T}$$

where  $P_L$ ,  $P_N$  and  $P_T$  are respectively the longitudinal, normal and transverse components of  $\mathbf{P}$  in the resonance rest frame [8, 9].

### 2.2.2 T-odd Observables

Since the spin of any particle is T-odd, studying its mean value or its polarization provides interesting tool to test Time-Reversal symmetry violation.

observable	<b>T</b>
$\vec{e}_X$	-
$\vec{e}_Y$	-
$\vec{e}_Z$	+
$\mathbf{P}^{\Lambda_c}$	-
$P_X^{\Lambda_c}$	+
$P_Y^{\Lambda_c}$	+
$P_Z^{\Lambda_c}$	-

Table 2.1: Effect of Time-Reversal transformation on  $\Lambda_c^+$  polarization-vector

observable	<b>T</b>
$\vec{e}_L$	-
$\vec{e}_T$	-
$\vec{e}_N$	+
$\mathbf{P}^R$	-
$P_L^R$	+
$P_T^R$	+
$P_N^R$	-

Table 2.2: Effect of Time-Reversal transformation on resonance polarization-vector

Therefore according to the result of the Table 2.1 and Table 2.2, if  $P_Z^{\Lambda_c} \neq 0$  or  $P_N^{\Lambda} \neq 0$ , we have a sign of Time-Reversal symmetry violation (Wolfenstein Theorem, 2000).

## 2.3 Calculation of the Angular Distributions

We have the following total decay process:

$$\Lambda_c^+ \rightarrow \Lambda W^+ \rightarrow p \pi^- \mu^+ \nu_\mu$$

### 2.3.1 Initial Resonance Decay: $\Lambda_c^+(M_i) \rightarrow \Lambda(\lambda_1)W^+(\lambda_2)$

By applying the Wigner-Eckart theorem to the S-matrix element in the framework of the Jacob-Wick helicity formalism, the analytic form of the decay amplitude is expressed as [6, 10]:

$$A_0(M_i) = M_{\Lambda_c}(\lambda_1, \lambda_2) D_{M_i, M_f}^{1/2*}(\phi, \theta, 0)$$

where:

- $M_i = \pm 1/2$  represents the projection of the initial spin of  $\Lambda_c^+$  along the quantization axis  $\vec{\Lambda}_c^+ \vec{Z}$ .
- $\lambda_1 = \pm 1/2$  and  $\lambda_2 = +1, 0, -1$  are the possible helicities of the  $\Lambda$  and of the  $W^+$  respectively.
- $M_f = \lambda_1 - \lambda_2 = \pm 1/2$ . It is the projection of the total angular momentum along the ( $\Delta$ ) axis (parallel to  $\vec{p}_\Lambda$ ). It constrains those of  $\lambda_1$  and  $\lambda_2$  since, among 6 combinations, only 4 are physical:  $(1/2, 1)$ ,  $(-1/2, 0)$ ,  $(1/2, 0)$ ,  $(-1/2, -1)$ .
- $M_{\Lambda_c}(\lambda_1, \lambda_2)$ : Hadronic Matrix element which contains all the decay dynamics.
- $D_{M_i, M_f}^j(\phi, \theta, 0)$ : Wigner Matrix related to the kinematics. It is expressed according to the Jackson convention as:

$$D_{M_i, M_f}^j(\phi, \theta, 0) = d_{M_i, M_f}^j(\theta) \exp(-i M_i \phi)$$

This decay amplitude must include all the possible intermediate states, thus a sum over the helicity states  $(\lambda_1, \lambda_2)$  must be performed. We define:

$$A_I = \sum_{\lambda_1, \lambda_2} A_0(M_i) = \sum_{\lambda_1, \lambda_2} M_{\Lambda_c}(\lambda_1, \lambda_2) d_{M_i, M_f}^{1/2}(\theta) \exp(i M_i \phi)$$

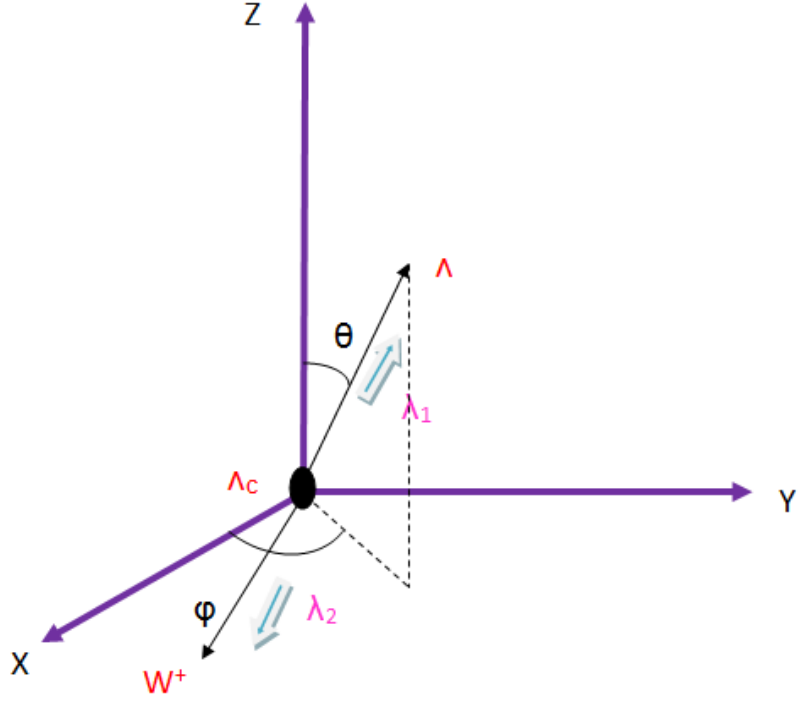


Figure 2.2:  $\Lambda_c^+$  rest frame

Since the initial spin component of  $\Lambda_c^+$  is unknown, we must introduce the polarization density matrix  $\rho^{\Lambda_c}$  in the following form:

$$d\sigma(\theta, \phi) \propto \sum_{M_i, M'_i} \rho_{M_i, M'_i}^{\Lambda_c} A_I A_I^*$$

After the summation over the possible helicity couples  $(\lambda_1, \lambda_2)$ :  $(1/2, 1)$   $(-1/2, 0)$   $(1/2, 0)$   $(-1/2, -1)$  and the summation over  $M_i, M'_i$  we get:

$$d\sigma(\theta, \phi) \propto |M_{\Lambda_c}(1/2)|^2 (\rho_{++}^{\Lambda_c} \cos^2(\theta/2) + \rho_{--}^{\Lambda_c} \sin^2(\theta/2) + \text{Re}(\rho_{+-}^{\Lambda_c} \exp(-i\phi) \sin \theta) \\ + |M_{\Lambda_c}(-1/2)|^2 (\rho_{++}^{\Lambda_c} \cos^2(\theta/2) + \rho_{--}^{\Lambda_c} \sin^2(\theta/2) + \text{Re}(\rho_{+-}^{\Lambda_c} \exp(-i\phi) \sin \theta))$$

where

$$|M_{\Lambda_c}(1/2)|^2 = |M_{\Lambda_c}(1/2, 0)|^2 + |M_{\Lambda_c}(-1/2, -1)|^2$$

and

$$|M_{\Lambda_c}(-1/2)|^2 = |M_{\Lambda_c}(-1/2, 0)|^2 + |M_{\Lambda_c}(1/2, 1)|^2$$

Noticing that  $\rho_{++}^{\Lambda_c} + \rho_{--}^{\Lambda_c} = 1$  and  $\rho_{++}^{\Lambda_c} - \rho_{--}^{\Lambda_c} = P_Z^{\Lambda_c}$  and  $\cos^2(\theta/2) = \frac{1}{2}(1 + \cos \theta)$ ,  $\sin^2(\theta/2) = \frac{1}{2}(1 - \cos \theta)$ , the above relation will become:

$$d\sigma(\theta, \phi) \propto |M_{\Lambda_c}(1/2)|^2 (1 + P_Z^{\Lambda_c} \cos \theta + \text{Re}(\rho_{+-}^{\Lambda_c} \exp(-i\phi) \sin \theta)) \\ + |M_{\Lambda_c}(-1/2)|^2 (1 - P_Z^{\Lambda_c} \cos \theta - \text{Re}(\rho_{+-}^{\Lambda_c} \exp(-i\phi) \sin \theta))$$

Because of parity violation,  $|M_{\Lambda_c}(1/2)|^2 \neq |M_{\Lambda_c}(-1/2)|^2$ , it is clearly seen that  $d\sigma(\theta, \phi) \neq d\sigma(\pi - \theta, \pi + \phi)$ . This property is put into evidence by introducing the asymmetry parameter  $\alpha_{AS}^{\Lambda_c}$  defined by:

$$\alpha_{AS}^{\Lambda_c} = \frac{|M_{\Lambda_c}(1/2)|^2 - |M_{\Lambda_c}(-1/2)|^2}{|M_{\Lambda_c}(1/2)|^2 + |M_{\Lambda_c}(-1/2)|^2}$$

Therefore, the angular distribution of  $\Lambda$  in the rest frame of  $\Lambda_c^+$  (Figure 2.2) will be expressed as:

$$\begin{aligned} \frac{d\sigma}{d\Omega} &\propto 1 + \alpha_{AS}^{\Lambda_c} P_Z^{\Lambda_c} \cos \theta_\Lambda + 2\alpha_{AS}^{\Lambda_c} \text{Re}[\rho_{+-}^{\Lambda_c} \exp(i\phi_\Lambda)] \sin \theta_\Lambda \\ &\propto 1 + \alpha_{AS}^{\Lambda_c} \mathbf{P}^{\Lambda_c} \cdot \mathbf{p}_\Lambda \end{aligned} \quad (2.1)$$

- The polar distribution according to  $\cos \theta$  of  $\Lambda$  :

$$\frac{d\sigma}{d \cos \theta_\Lambda} \propto 1 + \alpha_{AS}^{\Lambda_c} P_Z^{\Lambda_c} \cos \theta_\Lambda$$

- The azimuthal distribution according to  $\phi$  of  $\Lambda$  :

$$\frac{d\sigma}{d\phi_\Lambda} \propto 1 + \frac{\pi}{2} \alpha_{AS}^{\Lambda_c} \text{Re}[\rho_{+-}^{\Lambda_c} \exp(i\phi_\Lambda)]$$

### 2.3.2 Decay 1: $\Lambda(\lambda_1) \rightarrow P(\lambda_3)\pi^-(\lambda_4)$

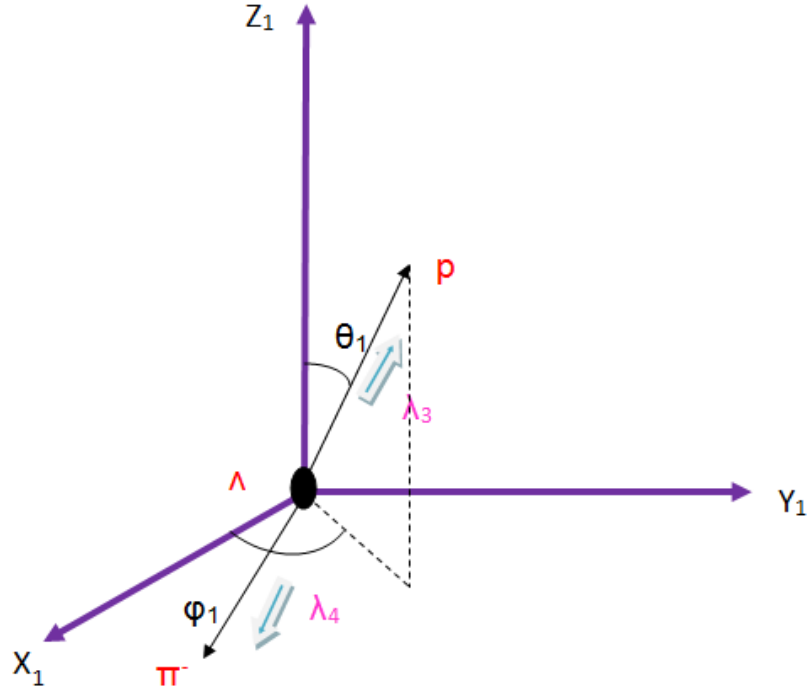


Figure 2.3:  $\Lambda$  rest frame



The general formula of the proton angular distribution in the  $\Lambda$  rest frame (Figure 2.3) is [6, 10]:

$$d\sigma(\theta_1, \phi_1) \propto \sum_{\lambda_1, \lambda'_1} \rho_{\lambda_1, \lambda'_1}^\Lambda A_I A_I^*$$

where

$$A_I = \sum_{\lambda_3} A_1(\lambda_1) = \sum_{\lambda_3} M_\Lambda(\lambda_3, 0) d_{\lambda_1, M_f}^{1/2}(\theta_1) \exp(i\lambda_1 \phi_1) \text{ such that } M_f = \lambda_3 - \lambda_4 (\lambda_4 = 0) = \pm 1/2$$

$\lambda_4 = 0$  since the spin of the pion is zero. By following the same mathematical technique as above; after the summation over the possible helicity couples  $(\lambda_3, 0)$ :  $(1/2, 0)$   $(-1/2, 0)$  and the summation over  $\lambda_1, \lambda'_1$  we get:

$$\begin{aligned} \frac{d\sigma}{d\Omega_1} &\propto 1 + \alpha_{AS}^\Lambda P_Z^\Lambda \cos \theta_p + 2\alpha_{AS}^\Lambda \mathcal{R}[\rho_{+-}^\Lambda \exp(i\phi_p)] \sin \theta_p \\ &\propto 1 + \alpha_{AS}^\Lambda \mathbf{P}^\Lambda \cdot \mathbf{p}_p \end{aligned} \quad (2.2)$$

where

$$\alpha_{AS}^\Lambda = \frac{|M_\Lambda(1/2)|^2 - |M_\Lambda(-1/2)|^2}{|M_\Lambda(1/2)|^2 + |M_\Lambda(-1/2)|^2}$$

and

$$P_Z^\Lambda = \rho_{++}^\Lambda - \rho_{--}^\Lambda$$

Studying  $\Lambda \rightarrow P\pi^-$  coming from  $\Lambda_c^+$  decays give us the opportunity to deduce the PDM of the  $\Lambda$  since its production mechanism is known. We obtain:

- $\rho_{++}^\Lambda = \frac{|M_{\Lambda_c}(1/2, 0)|^2 + |M_{\Lambda_c}(1/2, 1)|^2}{|M_{\Lambda_c}(1/2, 0)|^2 + |M_{\Lambda_c}(1/2, 1)|^2 + |M_{\Lambda_c}(-1/2, 0)|^2 + |M_{\Lambda_c}(-1/2, -1)|^2}$
- $\rho_{--}^\Lambda = \frac{|M_{\Lambda_c}(-1/2, 0)|^2 + |M_{\Lambda_c}(-1/2, -1)|^2}{|M_{\Lambda_c}(1/2, 0)|^2 + |M_{\Lambda_c}(1/2, 1)|^2 + |M_{\Lambda_c}(-1/2, 0)|^2 + |M_{\Lambda_c}(-1/2, -1)|^2}$
- $\rho_{+-}^\Lambda = -\frac{\pi}{4} \frac{|M_{\Lambda_c}(1/2, 0)| |M_{\Lambda_c}(-1/2, 0)|^*}{|M_{\Lambda_c}(1/2, 0)|^2 + |M_{\Lambda_c}(1/2, 1)|^2 + |M_{\Lambda_c}(-1/2, 0)|^2 + |M_{\Lambda_c}(-1/2, -1)|^2} P_Z^{\Lambda_c}$
- $\rho_{-+}^\Lambda = \rho_{+-}^{\Lambda*}$

We notice that the initial polarization of  $\Lambda_c^+$  along the  $\vec{OZ}$  axis appears in the  $\rho_{+-}^\Lambda$  element. Thus it is confirmed that the  $\Lambda_c^+$  decay mechanism is reflected in the polarization density matrix of  $\Lambda$ . The density matrix elements can be calculated by the aid of form factors related to a specific dynamics model [11].

### 2.3.3 Decay 2: $W^+(\lambda_2) \rightarrow \mu^+(\lambda_5) \nu_\mu(\lambda_6)$

The general formula of the lepton angular distribution in the  $W^+$  rest frame (Figure 2.4) is [6, 10]:

$$d\sigma(\theta_2, \phi_2) \propto \sum_{\lambda_2, \lambda'_2} \rho_{\lambda_2, \lambda'_2}^W A_I A_I^*$$

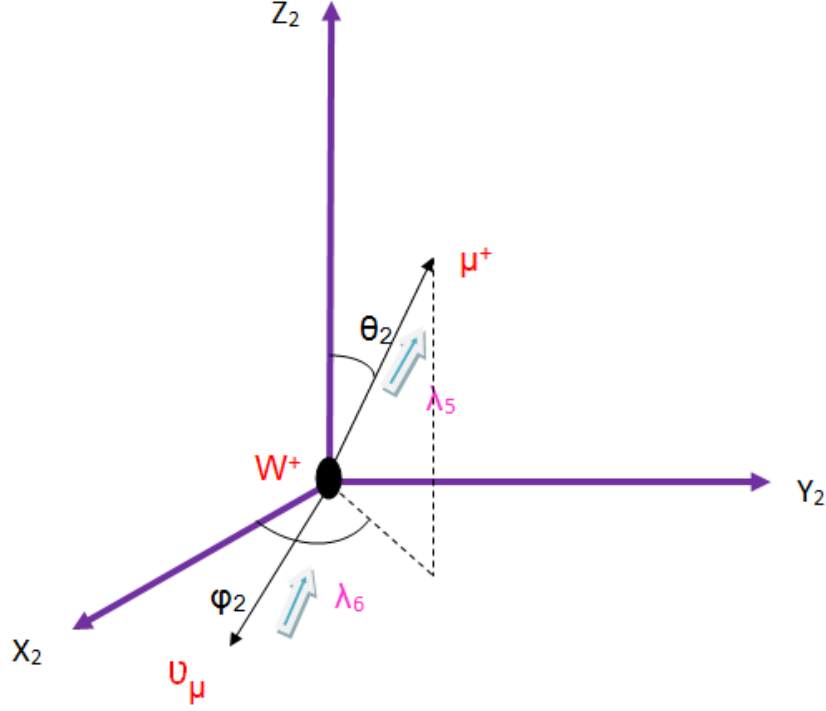


Figure 2.4:  $W^+$  rest frame

where

$$A_I = \sum_{\lambda_5} A_1(\lambda_2) = \sum_{\lambda_5} M_W(\lambda_5, -1/2) d_{\lambda_2, M_f}^1(\theta_2) \exp(i\lambda_2\phi_2) \text{ such that } M_f = \lambda_5 - \lambda_6 = \pm 1/2$$

$\lambda_6 = -1/2$ , since neutrinos are left-handed particles. By following the same mathematical technique as above; after the summation over the possible helicity couples  $(\lambda_4, -1/2)$ :  $(1/2, -1/2)$   $(-1/2, -1/2)$  and the summation over  $\lambda_2, \lambda'_2$  we get:

$$\begin{aligned} \frac{d\sigma}{d\Omega_2} \propto & \rho_{11}^W (|M_W(+ -)|^2 \frac{(1 + \cos \theta_2)^2}{4} + |M_W(- -)|^2 \frac{\sin^2 \theta_2}{2}) \\ & + 2\text{Re}(\rho_{10}^W \exp(i\phi_2)) (|M_W(+ -)|^2 \frac{\cos^2 \theta_2}{2} - |M_W(- -)|^2) \cos \theta_2 \frac{\sin \theta_2}{\sqrt{2}} \\ & + 2\text{Re}(\rho_{1-1}^W \exp(i2\phi_2)) (\frac{|M_W(+ -)|^2}{4} - \frac{|M_W(- -)|^2}{2}) \sin^2 \theta_2 \\ & + \rho_{00}^W (\frac{|M_W(+ -)|^2}{2} \sin^2 \theta_2 + |M_W(- -)|^2 \cos^2 \theta_2) \\ & + 2\text{Re}(\rho_{0-1}^W \exp(i\phi_2)) (|M_W(+ -)|^2 \frac{(1 - \cos \theta_2)^2}{2} + |M_W(- -)|^2 \cos \theta_2) \frac{\sin \theta_2}{\sqrt{2}} \\ & + \rho_{-1-1}^W (|M_W(+ -)|^2 \frac{(1 - \cos \theta_2)^2}{4} + |M_W(- -)|^2 \frac{\sin^2 \theta_2}{2}) \end{aligned} \quad (2.3)$$

It is in agreement with the results obtained by C.QUIGG [12] for specific polarization of the  $W^+$ ; particularly, for  $P_W^Z = +1, 0, -1$  where:

For helicity = 0 (completely longitudinally polarized);

$$\frac{d\sigma}{d\Omega} = \frac{G_F M_W^3}{6\pi\sqrt{2}} \sin^2 \theta_2$$

For helicity = +1 (completely transversely polarized with the direction of quantization axis) ;

$$\frac{d\sigma}{d\Omega} = \frac{G_F M_W^3}{32\pi^2\sqrt{2}} (1 + \cos \theta_2)^2$$

For helicity = -1 (completely transversely polarized opposite to direction of quantization axis) ;

$$\frac{d\sigma}{d\Omega} = \frac{G_F M_W^3}{32\pi^2\sqrt{2}} (1 - \cos \theta_2)^2$$

Again from  $\Lambda_c^+$  decay amplitude, we can deduce the PDM of the  $W^+$ :

- $\rho_{11}^W = \frac{|M_{\Lambda_c}(1/2,1)|^2}{|M_{\Lambda_c}(1/2,0)|^2 + |M_{\Lambda_c}(1/2,1)|^2 + |M_{\Lambda_c}(-1/2,0)|^2 + |M_{\Lambda_c}(-1/2,-1)|^2}$
- $\rho_{00}^W = \frac{|M_{\Lambda_c}(1/2,0)|^2 + |M_{\Lambda_c}(-1/2,0)|^2}{|M_{\Lambda_c}(1/2,0)|^2 + |M_{\Lambda_c}(1/2,1)|^2 + |M_{\Lambda_c}(-1/2,0)|^2 + |M_{\Lambda_c}(-1/2,-1)|^2}$
- $\rho_{-1-1}^W = \frac{|M_{\Lambda_c}(-1/2,-1)|^2}{|M_{\Lambda_c}(1/2,0)|^2 + |M_{\Lambda_c}(1/2,1)|^2 + |M_{\Lambda_c}(-1/2,0)|^2 + |M_{\Lambda_c}(-1/2,-1)|^2}$
- $\rho_{10}^W = -\frac{\pi}{4} \frac{|M_{\Lambda_c}(1/2,1)|^2 |M_{\Lambda_c}(1/2,0)|^2}{|M_{\Lambda_c}(1/2,0)|^2 + |M_{\Lambda_c}(1/2,1)|^2 + |M_{\Lambda_c}(-1/2,0)|^2 + |M_{\Lambda_c}(-1/2,-1)|^2} P_Z^{\Lambda_c}$
- $\rho_{1-1}^W = 0$
- $\rho_{0-1}^W = -\frac{\pi}{4} \frac{|M_{\Lambda_c}(-1/2,0)|^2 |M_{\Lambda_c}(-1/2,-1)|^2}{|M_{\Lambda_c}(1/2,0)|^2 + |M_{\Lambda_c}(1/2,1)|^2 + |M_{\Lambda_c}(-1/2,0)|^2 + |M_{\Lambda_c}(-1/2,-1)|^2} P_Z^{\Lambda_c}$

It is worthy noticing that:

$$\rho_{01}^W = \rho_{10}^{*W} \quad \rho_{-11}^W = \rho_{-11}^{*W} \quad \rho_{-10}^W = \rho_{0-1}^{*W}$$

We notice again that the initial polarization of  $\Lambda_c^+$  appears in the  $\rho_{10}^W$  and  $\rho_{0-1}^W$  elements. The density matrix elements can be estimated by the aid of specific form factors [11].

# Chapter 3

## Simulations

Simulations are important in order to be as close as possible to the physical reality.

### 3.1 Kinematics of the Decay $\Lambda_c^+ \rightarrow \Lambda \mu^+ \nu_\mu$

#### 3.1.1 Three-Body Decay Process

Consider the following three-body decay process:

$$\Lambda_c^+ \rightarrow \Lambda \mu^+ \nu_\mu \quad (3.1)$$

How many free parameters do we need to perform Monte Carlo simulations ?

It is convenient to regard this decay process as a quasi two-body decay  $\Lambda_c^+ \rightarrow \Lambda W^+$  followed by the leptonic decay  $W^+ \rightarrow \mu^+ \nu_\mu$  where  $W^+$  is a virtual boson [7].

$P_{\Lambda_c} = P_\Lambda + P_\mu + P_{\nu_\mu} \rightarrow 12$  unknown parameters.

$M_{\Lambda_c} = E_\Lambda + E_\mu + E_{\nu_\mu} \rightarrow 1$  constraint.

$0 = \mathbf{p}_\Lambda + \mathbf{p}_\mu + \mathbf{p}_{\nu_\mu} \rightarrow 3$  constraints.

$E_\Lambda = \sqrt{\mathbf{p}_\Lambda^2 + m_\Lambda^2}$  ,  $E_\mu = \sqrt{\mathbf{p}_\mu^2 + m_\mu^2}$  ,  $E_{\nu_\mu} = \sqrt{\mathbf{p}_{\nu_\mu}^2 + m_{\nu_\mu}^2} \rightarrow 3$  constraints.

Thus,

$$\begin{aligned} \text{free parameters} &= \text{total number of unknown parameters} - \text{total number of constraints} \\ &= 12 - 7 \\ &= 5. \end{aligned}$$

First, take the initial resonance decay  $\Lambda_c^+ \rightarrow \Lambda W^+$ . By applying the energy-momentum conservation in the  $\Lambda_c^+$  rest frame:

$$\begin{aligned} M_{\Lambda_c} &= E_\Lambda + E_W \\ 0 &= \mathbf{p}_\Lambda + \mathbf{p}_W \rightarrow \mathbf{p}_\Lambda = -\mathbf{p}_W \quad (\text{Figure 3.1}) \end{aligned}$$

The lepton pair does not originate from a resonance with a given mass, but from a virtual W-boson whose mass is not fixed. In this case, an additional parameter arises which is the invariant mass of the  $(\mu^+\nu_\mu)$  system denoted by  $q_W$ .

We have:

$$\begin{aligned}
P_{\Lambda_c} &= P_\Lambda + P_W \rightarrow P_W^2 = (P_{\Lambda_c} - P_\Lambda)^2 \\
&= P_{\Lambda_c}^2 + P_\Lambda^2 - 2P_{\Lambda_c}P_\Lambda \\
&= M_{\Lambda_c}^2 + m_\Lambda^2 - 2P_{\Lambda_c}P_\Lambda \\
&= q_W^2
\end{aligned} \tag{3.2}$$

Then,  $E_\Lambda$ , the energy of the  $\Lambda$  in  $\Lambda_c$  rest frame can be deduced:

$$E_\Lambda = \frac{M_{\Lambda_c}^2 + m_\Lambda^2 - q_W^2}{2M_{\Lambda_c}}$$

The energy of  $W^+$  in the rest frame of  $\Lambda_c$  is calculated in a similar way:

$$E_W = \frac{M_{\Lambda_c}^2 + q_W^2 - m_\Lambda^2}{2M_{\Lambda_c}}$$

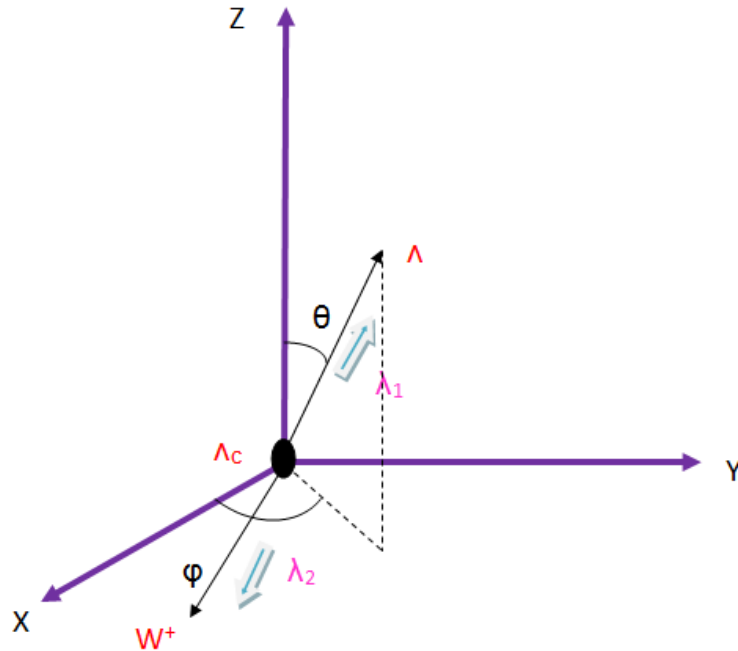


Figure 3.1:  $\Lambda_c^+$  decay in its rest frame

Thus, the quadrivector momentums for both  $\Lambda$  and  $W^+$  are respectively:

$$P_\Lambda = \begin{pmatrix} \frac{M_{\Lambda_c}^2 + m_\Lambda^2 - q_W^2}{2M_{\Lambda_c}} \\ |\mathbf{p}_\Lambda| \sin \theta \cos \phi \\ |\mathbf{p}_\Lambda| \sin \theta \sin \phi \\ |\mathbf{p}_\Lambda| \cos \theta \end{pmatrix} \quad \text{and} \quad P_W = \begin{pmatrix} \frac{M_{\Lambda_c}^2 + q_W^2 - m_\Lambda^2}{2M_{\Lambda_c}} \\ -|\mathbf{p}_\Lambda| \sin \theta \cos \phi \\ -|\mathbf{p}_\Lambda| \sin \theta \sin \phi \\ -|\mathbf{p}_\Lambda| \cos \theta \end{pmatrix}$$

Next, in the  $W^+$  rest frame, the following process  $W^+ \rightarrow \mu^+ \nu_\mu$  is studied. By using the same previous mathematical technique, the quadrivector momentums for both  $\mu^+$  and  $\nu_\mu$  are respectively:

$$P_\mu = \begin{pmatrix} \frac{q_W^2 + m_{\mu^+}^2 - m_{\nu_\mu}^2}{2q_W} \\ |\mathbf{p}_\mu| \sin \theta_2 \cos \phi_2 \\ |\mathbf{p}_\mu| \sin \theta_2 \sin \phi_2 \\ |\mathbf{p}_\mu| \cos \theta_2 \end{pmatrix} \quad \text{and} \quad P_{\nu_\mu} = \begin{pmatrix} \frac{q_W^2 + m_{\nu_\mu}^2 - m_{\mu^+}^2}{2q_W} \\ -|\mathbf{p}_\mu| \sin \theta_2 \cos \phi_2 \\ -|\mathbf{p}_\mu| \sin \theta_2 \sin \phi_2 \\ -|\mathbf{p}_\mu| \cos \theta_2 \end{pmatrix}$$

As a result, 5 free parameters must be generated which are:  $\phi, \cos \theta, \phi_2, \cos \theta_2, q_W^2$ . The mass of the muon neutrino has been taken to be 0.5 Mev.

If we take into account the decay process  $\Lambda \rightarrow p \pi^-$ , two more parameters will be added ( $\phi_1, \cos \theta_1$ ) of p in the  $\Lambda$  rest frame. So in order to perform a full simulations of the channel:

$\Lambda_c^+ \rightarrow \Lambda W^+ \rightarrow p \pi^- \mu^+ \nu_\mu$ , we need 7 parameters which are  $\phi, \cos \theta, \phi_2, \cos \theta_2, q_W^2, \phi_1, \cos \theta_1$ .

## 3.2 Monte-Carlo Simulations

### 3.2.1 Step 1

By using the C++ language, we generate uniformly the 7 parameters indicated above, where:

$$\begin{aligned} -1 &< \cos \theta < +1 \\ 0 &< \phi < 2\pi \\ -1 &< \cos \theta_1 < +1 \\ 0 &< \phi_1 < 2\pi \\ -1 &< \cos \theta_2 < +1 \\ 0 &< \phi_2 < 2\pi \\ m_\mu^2 &< q_W^2 < (M_{\Lambda_c} - m_\Lambda)^2 \end{aligned}$$

where:

$$M_{\Lambda_c} = 2286.46 \text{ Mev}$$

$$m_\Lambda = 1115.683 \text{ Mev}$$

$$m_\mu = 105.658 \text{ Mev}$$

The distribution of the quadrivector momentums for both  $\mu^+$  and  $\nu_\mu$  in the  $W^+$  rest frame and the ones of both p and  $\pi^-$  in the  $\Lambda$  rest frame are found. Applying Lorentz transformation  $\vec{\beta}_W = \frac{\vec{p}_W}{E_W}$  and  $\vec{\beta}_\Lambda = \frac{\vec{p}_\Lambda}{E_\Lambda}$  in to  $(\mu^+ \nu_\mu)$  and  $(p \pi^-)$  systems respectively, one can pass these quantities to the  $\Lambda_c^+$  rest frame.

### 3.2.2 Step 2

The equation (2.1) in Chapter 2 represents the total angular distribution of the  $\Lambda$  in the  $\Lambda_c^+$  rest frame, and it enables us to deduce:

- 1) The polar angular distribution of  $\Lambda$  in  $\Lambda_c^+$  rest frame:

$$\frac{d\sigma}{d\cos\theta_\Lambda} \propto 1 + \alpha_{AS}^{\Lambda_c} P_Z^{\Lambda_c} \cos\theta_\Lambda$$

By using the PDG,  $\alpha_{AS}^{\Lambda_c} = -0.86$  [13]. The polar distribution according to  $\cos\theta_\Lambda$  is given below for different values of  $\Lambda_c^+$  polarization:

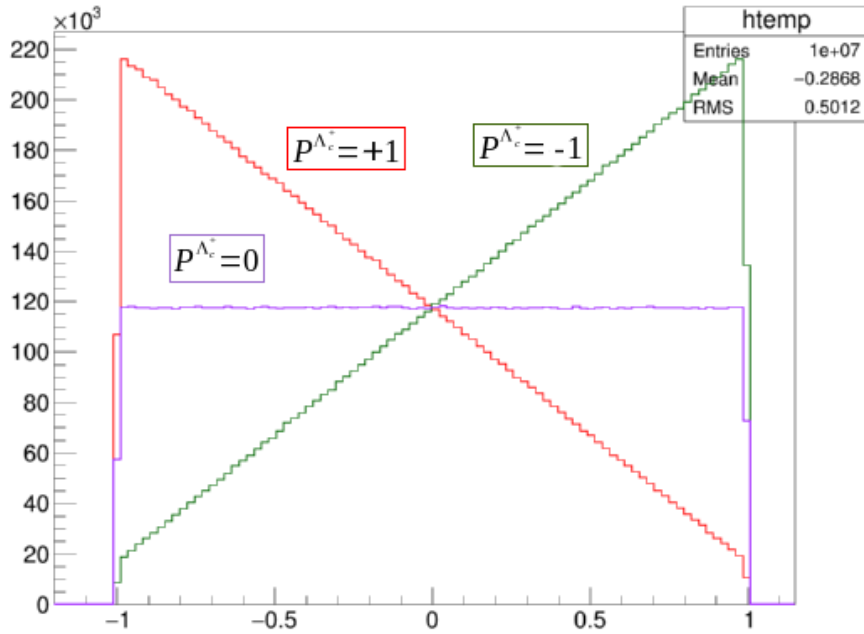


Figure 3.2: Angular distribution according to  $\cos\theta_\Lambda$  in  $\Lambda_c^+$  rest frame for different  $P_Z^{\Lambda_c}$

Remarks:

- The distribution according to  $\cos\theta_\Lambda$  is linear with  $P_Z^{\Lambda_c}$ . Thus the distribution is said to be uniform when  $\Lambda_c^+$  is unpolarized, or in other words  $P_Z^{\Lambda_c}=0$ .
- For  $P_Z^{\Lambda_c} = +1$  ( $\Lambda_c^+$  is said to be totally polarized along the quantization axis) the distribution is linear of the form  $(\frac{d\sigma}{d\cos\theta_\Lambda} \propto 1-0.86\cos\theta_\Lambda)$ .
- For  $P_Z^{\Lambda_c} = -1$  ( $\Lambda_c^+$  is totally polarized in the opposite direction of the quantization axis) the distribution is linear of the form  $(\frac{d\sigma}{d\cos\theta_\Lambda} \propto 1+0.86\cos\theta_\Lambda)$ .

- 2) The angular distribution according to  $\phi_\Lambda$  of the  $\Lambda$  in  $\Lambda_c^+$  rest frame:

$$\frac{d\sigma}{d\phi_\Lambda} \propto 1 + \frac{\pi}{2} \alpha_{AS}^{\Lambda_c} \text{Re}[\rho_{+-}^{\Lambda_c} \exp(i\phi_\Lambda)]$$

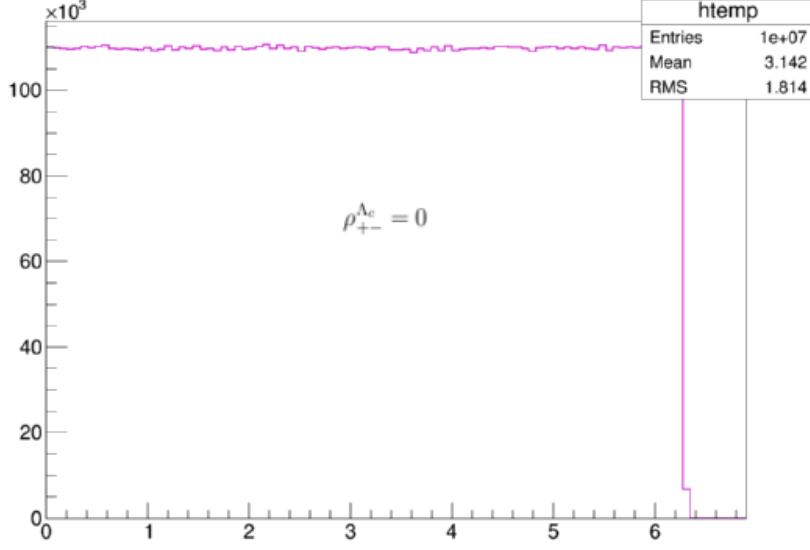


Figure 3.3: Angular distribution of  $\phi_\Lambda$  in  $\Lambda_c^+$  rest frame for  $\rho_{+-}^{\Lambda_c}=0$

The most interesting thing in the Figure 3.3 is that the distribution according to  $\phi_\Lambda$  does not depend on the vector-polarization component  $P_Z^{\Lambda_c}$  of  $\Lambda_c^+$ , but rather it depends on the other components;  $P_x^{\Lambda_c} = 2\text{Re}(\rho_{+-}^{\Lambda_c})$  and  $P_y = -2\text{Im}(\rho_{+-}^{\Lambda_c})$ . Because of the unknown values of  $\rho_{+-}^{\Lambda_c}$ , they are set to zero and the angular distribution according to  $\phi_\Lambda$  is uniform.

### 3.2.3 Step 3

In the  $W^+$  rest frame, the angular distribution of  $\mu^+$  is found to be:

$$\begin{aligned}
 \frac{d\sigma}{d\Omega_2} \propto & \rho_{11}^W (|M_W(+ -)|^2 \frac{(1 + \cos \theta_2)^2}{4} + |M_W(- -)|^2 \frac{\sin^2 \theta_2}{2}) \\
 & + 2\text{Re}(\rho_{10}^W \exp(i\phi_2)) (|M_W(+ -)|^2 \frac{\cos^2 \theta_2}{2} - |M_W(- -)|^2) \cos \theta_2 \frac{\sin \theta_2}{\sqrt{2}} \\
 & + 2\text{Re}(\rho_{1-1}^W \exp(i2\phi_2)) (\frac{|M_W(+ -)|^2}{4} - \frac{|M_W(- -)|^2}{2}) \sin^2 \theta_2 \\
 & + \rho_{00}^W (\frac{|M_W(+ -)|^2}{2} \sin^2 \theta_2 + |M_W(- -)|^2 \cos^2 \theta_2) \\
 & + 2\text{Re}(\rho_{0-1}^W \exp(i\phi_2)) (|M_W(+ -)|^2 \frac{(1 - \cos \theta_2)^2}{2} + |M_W(- -)|^2 \cos \theta_2) \frac{\sin \theta_2}{\sqrt{2}} \\
 & + \rho_{-1-1}^W (|M_W(+ -)|^2 \frac{(1 - \cos \theta_2)^2}{4} + |M_W(- -)|^2 \frac{\sin^2 \theta_2}{2})
 \end{aligned} \tag{3.3}$$

Supposing that the longitudinal polarization is dominant (  $\rho_{ij}^W$  negligible for  $i \neq j \neq 0$  ), we get:

$$\frac{d\sigma}{d\Omega_2} \propto \rho_{00}^W (\frac{|M_W(+ -)|^2}{2} \sin^2 \theta_2 + |M_W(- -)|^2 \cos^2 \theta_2) \quad \text{with} \quad \rho_{00}^W = 1$$

Supposing that the transverse polarization is dominant (  $\rho_{ij}^W$  negligible for  $i \neq j \neq 1$  ), we get:



$$\frac{d\sigma}{d\Omega_2} \propto \rho_{11}^W (|M_W(+ -)|^2 \frac{(1 + \cos \theta_2)^2}{4} + |M_W(- -)|^2 \frac{\sin^2 \theta_2}{2}) \quad \text{with} \quad \rho_{11}^W = 1$$

Supposing that the transverse polarization is dominant (  $\rho_{ij}^W$  negligible for  $i \neq j \neq -1$  ), we get:

$$\frac{d\sigma}{d\Omega_2} \propto \rho_{-1-1}^W (|M_W(+ -)|^2 \frac{(1 - \cos \theta_2)^2}{4} + |M_W(- -)|^2 \frac{\sin^2 \theta_2}{2}) \quad \text{with} \quad \rho_{-1-1}^W = 1$$

Dynamical hypothesis based on chirality assumes that  $|M_W(+ -)|^2 \gg |M_W(- -)|^2$ . So the angular distributions for the three polarization values of  $W^+$  are with agreement with those obtained by CHRIS QUIGG [12] which are as given below:

For complete longitudinal polarization:

$$\frac{d\sigma}{d\Omega} = \frac{G_F M_W^3}{6\pi\sqrt{2}} \sin^2 \theta_2$$

For complete transverse polarization with direction of the quantization axis ( $P_z^W = +1$ ):

$$\frac{d\sigma}{d\Omega} = \frac{G_F M_W^3}{32\pi^2\sqrt{2}} (1 + \cos \theta_2)^2$$

For complete transverse polarization opposite to the direction of quantization axis ( $P_z^W = -1$ ):

$$\frac{d\sigma}{d\Omega} = \frac{G_F M_W^3}{32\pi^2\sqrt{2}} (1 - \cos \theta_2)^2$$

By Monte-Carlo technique, the angular distributions according to  $\cos \theta_2$  for the three cases of  $W^+$  polarization are given below:

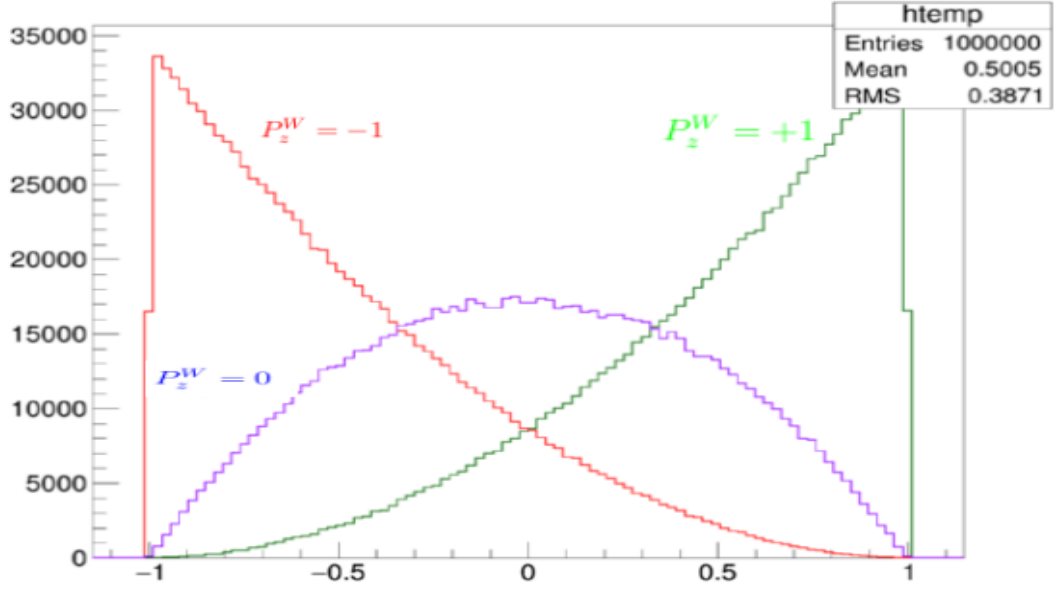


Figure 3.4: Distribution of  $\cos \theta_2$  in  $W^+$  rest frame for different values of  $P_z^W$

Remarks:

- The polar distribution according to  $\cos \theta_2$  of  $\mu^+$  in the  $W^+$  rest frame is independent on the initial polarization of the  $\Lambda_c^+$ .
- In case the W-boson is longitudinally polarized (i.e  $\rho_{00}^W = 1$ ), the angular distribution according to  $\cos \theta_2$  is proportional to  $1 - \cos^2 \theta_2 = \sin^2 \theta_2$ .
- Taking the W-boson to be totally polarized along the quantization axis ( $\rho_{11}^W = 1$ ), the polar distribution is proportional to  $(1 + \cos \theta_2)^2$ .
- In the case where W-boson is totally polarized in opposition to the quantization axis ( $\rho_{-1-1}^W = 1$ ), the polar distribution is proportional to  $(1 - \cos \theta_2)^2$ .
- In the three cases above, the angular distribution according to  $\phi_2$  is uniformly distributed.

In our simulations, three main values are chosen for the polarization of  $\Lambda_c^+$ : 0,+1,-1 and also three main values are chosen for the polarization of  $W^+$ : 0,+1,-1. In the  $\Lambda_c^+$  rest frame, the distribution of the invariant mass for the 9 cases where we combine both  $P_z^{\Lambda_c}$  and  $P_z^W$  are simulated for the system ( $\Lambda\mu^+$ ) which gives an overview concerning the selection process of the  $\Lambda_c^+$  with the real data. The distributions are given below which show mass distributions due to the missing energy and momentum vector of the neutrino:

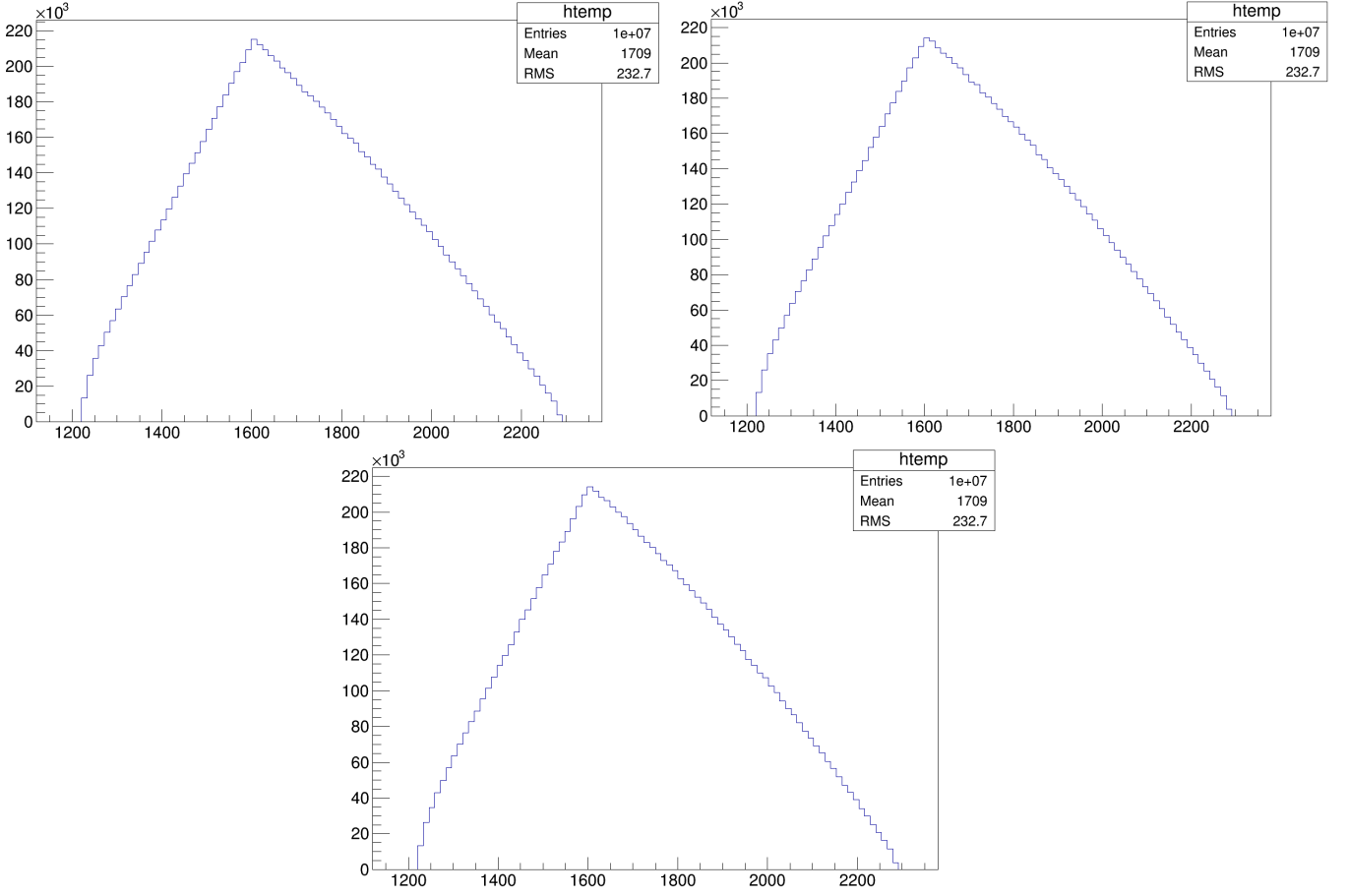


Figure 3.5:  $P_z^W=0$  and  $P_z^{\Lambda_c}=0,+1,-1$  respectively (right to left)

By analyzing the above three graphs, we notice that the distribution of the invariant mass of the detected system ( $\Lambda\mu^+$ ) does not vary for a given  $W^+$  polarization (completely longitudinally polarized;  $P_z^W=0$ ) among the three different polarization values of  $\Lambda_c^+$ .

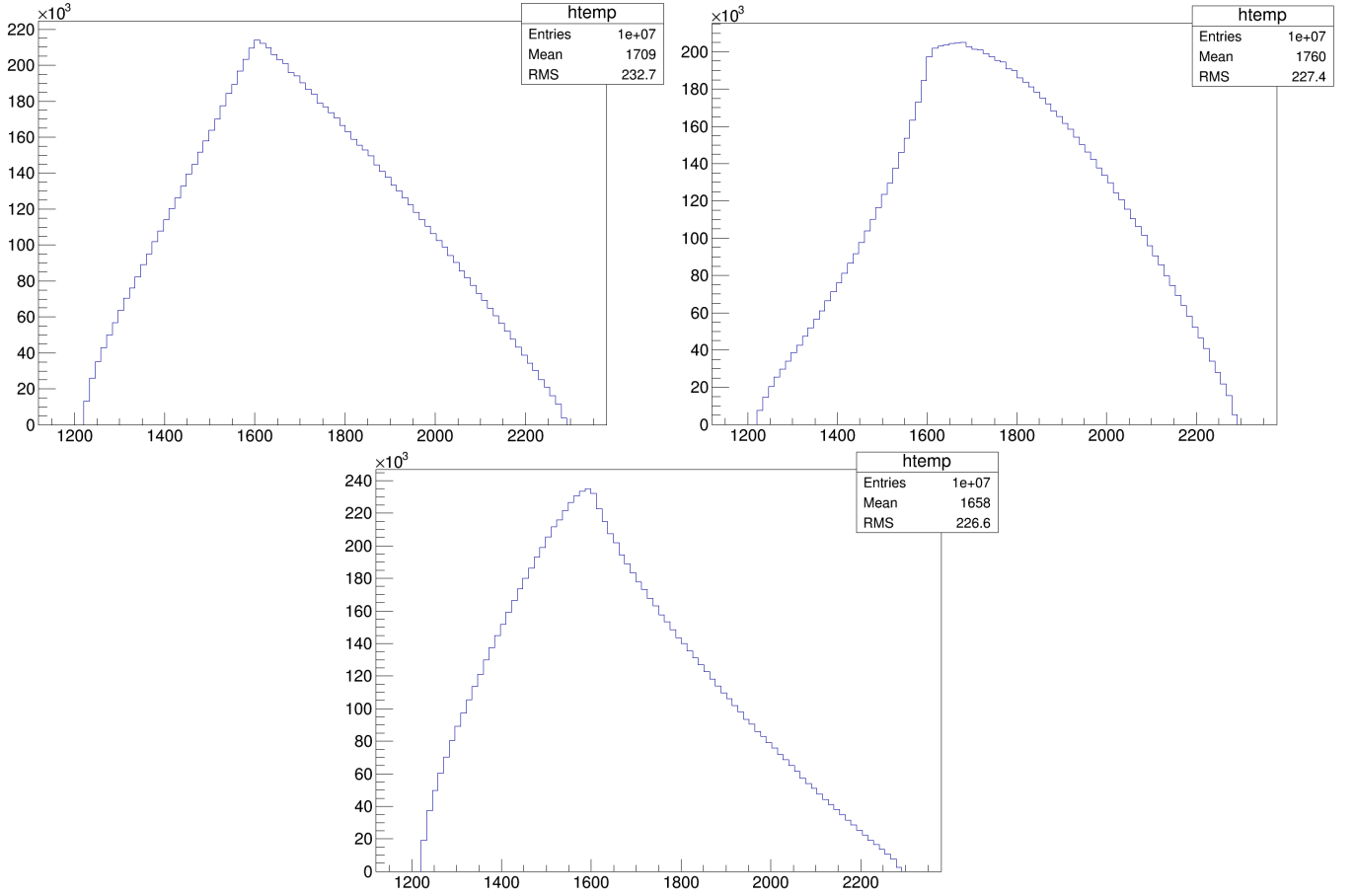


Figure 3.6:  $P_z^W=+1$  and  $P_z^{\Lambda_c}=0,+1,-1$  respectively (right to left)

The graphs corresponding to  $\Lambda_c^+$  polarization equal to -1 and that equal to +1 for a given  $W^+$  polarization ( transversely polarized along the direction of quantization axis ) are correlated.

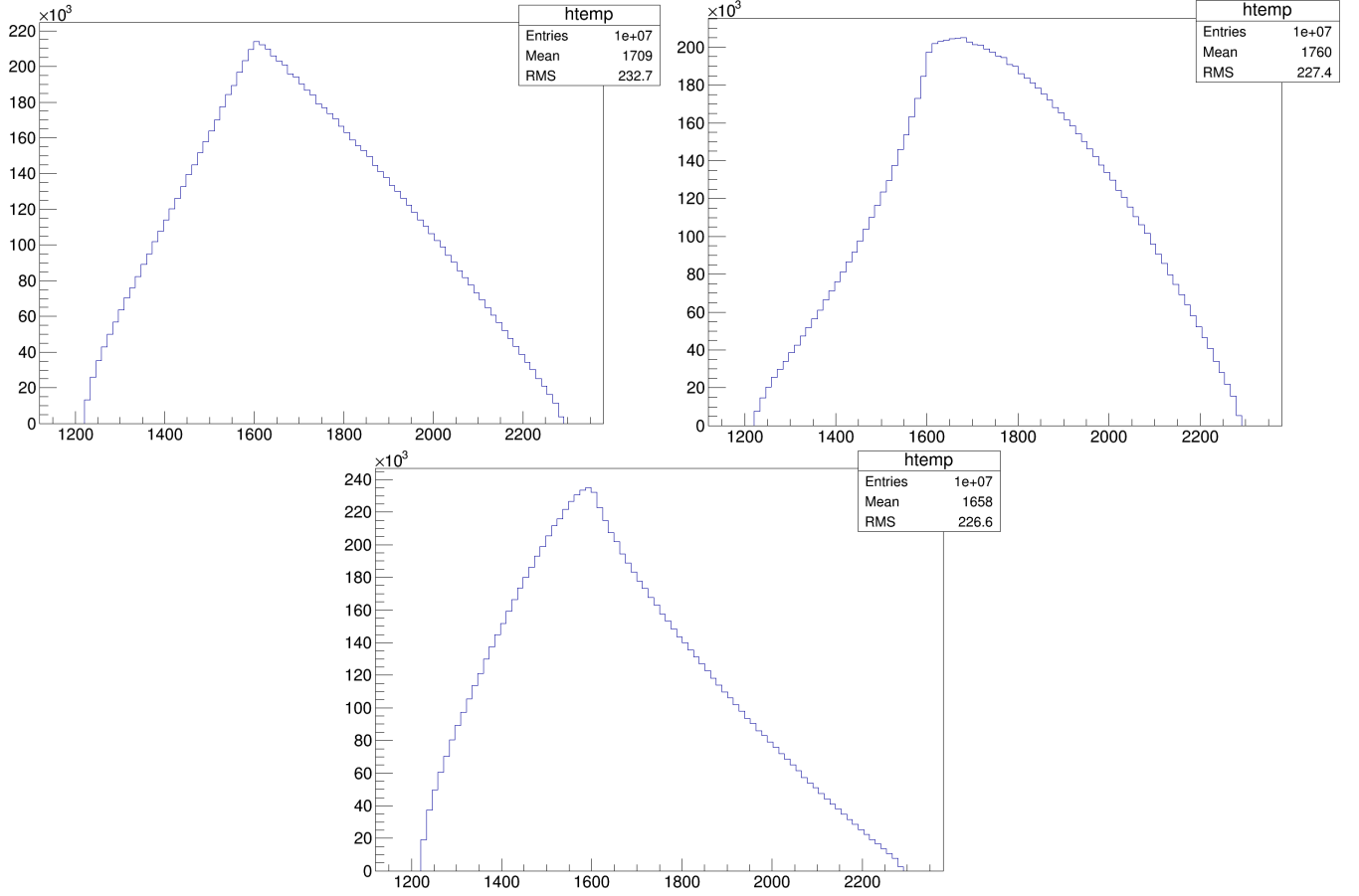


Figure 3.8:  $P_z^W = -1$  and  $P_z^{\Lambda_c} = 0, +1, -1$  respectively (right to left)

By comparing the previous graphs ( for  $W^+$  polarization equals  $+1$  ) with the above ones ( for  $W^+$  polarization equals  $-1$  ), we notice that the distribution of the invariant mass of the detected system ( $\Lambda_c^+$ ) is not affected by the variation of the  $W^+$  polarization for a given  $\Lambda_c^+$  polarization.

# Conclusion

As a part of our mission in the search for a direct Time-Reversal violation, the channel  $\Lambda_c^+ \rightarrow \Lambda \mu^+ \nu_\mu$ , with the approximation of quasi two-body decay, is studied. Complete calculations for the angular distributions based on the helicity formalism of the decay amplitude  $A(\Lambda_c^+ \rightarrow \Lambda \mu^+ \nu_\mu)$  have been performed. Owing to the polarization of the intermediate resonances  $\Lambda$  and  $W^+$ , it has shown that the normal components of their respective polarization-vectors are T-odd observables and must be taken as serious candidates to check Time-Reversal symmetry.

By using C++ language, the different angular distributions are generated by Monte-Carlo techniques as an approach to have an idea of their distribution form.

The elements of the resonances' PDM can be computed analytically, but their numerical values are unknown because they depend on form-factors which neither have been measured nor yet computed, situations which open the door for both future calculations and sophisticated simulations.

A new field of research beyond the Standard Model may be possible through the search for Time-Reversal violation effects in baryon decays.

# Bibliography

- [1] R.E. Marshak, Riazuddin, and P.R. Ciaran. *Theory Of Weak Interactions In Particle Physics*. Wiley-Interscience, 1969.
- [2] I.I. Bigi and A.I. Sanda. *CP violation*. Cambridge University Press, 2000.
- [3] Z.J. Ajaltouni, E. Di Salvo, and O. Leitner. Testing Time-Reversal:  $\Lambda_b$  Decays into Polarized Resonances.
- [4] R.H. Dalitz. The production and decay of resonant states. 1966.
- [5] Eugen Merzbacher. *Quantum Mechanics*. Wiley, 1997.
- [6] Z.J. Ajaltouni and E. Conte. Angular analysis of  $\Lambda_b$  decays into  $\Lambda V(1^-)$ : Applications to time-odd observables and CP violation in  $\Lambda_b$  decays (I). 2004.
- [7] J.G. Korner and M. Kramer. Polarization effects in exclusive semi-leptonic  $\Lambda_c$  and  $\Lambda_b$  charm and bottom baryon decays. *Physics Letters B*, 275(34):495 – 505, 1992.
- [8] Marwa Jahjah. Analyse du canal  $\Lambda_b \rightarrow \Lambda + J/\Psi$  et mesure de la polarisation du baryon  $\Lambda$  produit dans les collisions  $p - p$  7 TeV avec le dtecteur LHCb.
- [9] Z.J. Ajaltouni, E. Conte, and O. Leitner.  $\Lambda_b$  decays into  $\Lambda$ -vector. *Phys.Lett.*, B614:165–173, 2005.
- [10] J.D. Jackson. "Particle and polarization angular distribution for two and three-body decays". les houches(PP.325-366),1965.
- [11] Hai-Yang Cheng. "Charm baryon production and decays". *Int.J.Mod.Phys.*, A24S1:593–626, 2009.
- [12] C. Quigg. Gauge Theories of the Strong, Weak and Electromagnetic Interactions. *Front.Phys.*, 56:1–334, 1983.
- [13] K.A. Olive et al. Review of Particle Physics. *Chin.Phys.*, C38:090001, 2014.